

Energy loss and straggling for 50- and 100-keV H⁺ ions passing through the Si(001)2×1-Sb surface

Koji Sumitomo and Takashi Nishioka*

NTT Basic Research Laboratories, Atsugi, Kanagawa 243-01, Japan

Atsushi Ikeda and Yoshiaki Kido

Department of Physics, Ritsumeikan University, Kusatsu, Shiga 525-77, Japan

(Received 23 August 1996)

Surface stopping powers were measured for 50- and 100-keV H⁺ ions passing through the Si(001)2×1-Sb surface. The energy losses as a function of the exit angle are fit successfully by a simple relationship involving the time spent near the surface. The fitting parameter is in agreement with the value expected from the bulk Sb stopping cross section and the areal Sb density. This result suggests continuity of the stopping power from the bulk to the surface. It provides a useful method for determining the distance between the plane of deposited atoms and of a substrate surface and for measuring the composition of the topmost atomic layer. The estimated energy loss by surface-plasmon excitation is negligibly small in the present system. The energy straggling as a function of exit angle was also measured for 50- and 100-keV H⁺ incidence and the results are compared here with the bulk straggling values. [S0163-1829(97)04636-5]

I. INTRODUCTION

Medium-energy ion scattering (MEIS) with an electrostatic toroidal analyzer has been used to determine surface and interface atomic structures.¹⁻⁵ Ion shadowing and blocking provide quantitative information about surface reconstruction and relaxation and about crystallographic distortions at interfaces. The inelastic energy loss of ions passing through a surface region also provides information about the depth of an atomic layer. Glancing incidence or emergence geometry is often used in order to improve the depth resolution. Kimura, Ohshima, and Mannami⁶ derived a height of 0.05 ± 0.10 Å of Ag atoms on the Si(001) surface from the inelastic energy loss of backscattered He ions exiting at an angle of 3° from the surface. They calculated this height using Ziegler's stopping power formula⁷ and a theoretical prediction of the surface-plasmon loss.^{8,9}

Knowledge of the surface stopping powers is indispensable for determining the depth scale for atomic configurations near the surface. There are several reports on position-dependent stopping powers for light ions specularly reflected at atomically clean surfaces.¹⁰⁻¹³ A simple formula for the position-dependent stopping powers was derived from the analysis of the experimental data.¹⁰⁻¹³ Unfortunately, this formula is not applicable when the distance from the surface is less than about 0.5 Å. Theoretical investigations of surface energy-loss processes focus on the stopping power of a metal surface for ions traveling parallel to the surface.^{8,9,14} Kawai, Itoh, and Ohtsuki⁸ calculated the inelastic energy loss by collective excitations at a surface and derived a formula for the position-dependent stopping power.

In the present work, we measured the surface energy loss and straggling of 50- and 100-keV H⁺ ions passing through the Si(001)2×1-Sb surface as a function of exit angle. The surface atomic configuration has already been determined by surface-extended x-ray-absorption fine-structure analysis.¹⁵ To estimate the contributions from multiple scattering and

from backscattering from underlying substrate atoms, we calculated the backscattered ion trajectories using a Monte Carlo simulation. The contribution from surface-plasmon excitations is also discussed. The primary aim of the present work is to use the well-characterized surface to derive a relation between the surface and bulk stopping powers as well as the relation between surface and bulk energy straggling.

II. EXPERIMENTAL PROCEDURE

The experiments were performed in an ultrahigh vacuum (UHV) system, which consisted of three chambers for molecular-beam epitaxy (MBE), MEIS, and x-ray photoelectron spectroscopy. We prepared the samples in the MBE chamber and then transferred them to the MEIS chamber without exposing them to atmosphere. After the MEIS measurement, the samples were taken out of the UHV system and the surface morphology was studied with an atomic force microscope (AFM).

We preoxidized the surfaces of Si(001) wafers (B-doped, $\rho = 1-10$ Ω cm) by chemical treatment¹⁶ and then prepared the Si(001)2×1 surface by heating the sample to 900 °C under a base pressure of the order of 10^{-11} Torr. To get a flat and clean surface, a Si buffer layer with a thickness of about 200 Å was deposited at 500 °C using an electron gun evaporator and then we annealed the sample at 900 °C for a few minutes. The double domains of the dimer structure were confirmed by a clear 2×1 reflective high-energy electron diffraction pattern. From the step densities observed by AFM, we estimated the offset angle of the Si(001) wafer to be less than 0.02°. The Sb deposition was done with a Knudsen cell operating at 320 °C at a rate of about 1 ML/min, where 1 ML corresponds to 6.78×10^{14} cm⁻² of the ideal Si density of the (001) plane. Since the Si(001) substrate was kept at 680 °C during the Sb deposition, the Sb coverage was saturated at about 1 ML.¹⁷ We confirmed this 1-ML coverage by Ruthenium backscattering (RBS) with 1.0-MeV He⁺ ions. Three-

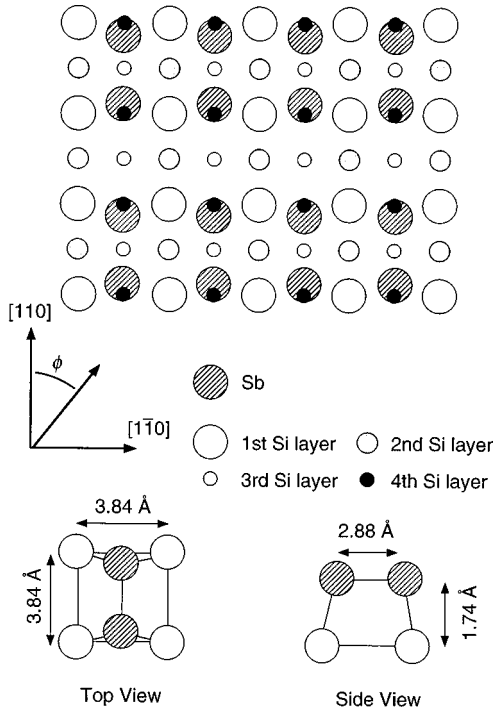


FIG. 1. Top and side view of the Si(001)2×1-Sb surface.

dimensional island formation was not observed in the AFM images. The schematic views of the single-domain Si(001)2×1-Sb surface^{15,18} are given in Fig. 1.

Well-collimated H⁺ beams were accelerated to 50.0 or 100.0 keV and were directed into the ultrahigh vacuum (UHV) MEIS chamber. The H⁺ ions were incident along the [001] axis. The energy of backscattered ions was analyzed with the electrostatic toroidal analyzer and collected by position sensitive microchannel plates with an acceptance angle of 25°. We measured the energy of the direct beam and confirmed the system energy resolution. The energy spectrum for the direct beam for 100-keV H⁺ was fit to a Gaussian shape with full width of half maximum (FWHM) of 340 eV. It also gave the basis of the energy scale with an accuracy of 30 eV. Two scattering planes were chosen: $\phi=0^\circ$ and 30° azimuth from the [110] axis, which correspond to the (110) scattering plane and to a random scattering plane, respectively. The incident and exit angles were calibrated with respect to the channeling and blocking directions and their accuracies are within $\pm 0.2^\circ$. To suppress surface damage induced by the probe ions, we moved the impact position on the sample surface, while keeping the scattering geometry unchanged.

Figure 2 shows a contour display of a typical MEIS spectra set around the Sb peak energies measured for 100.0-keV H⁺ incident along the Si-[001] axis of the Si(001)2×1-Sb. The product of the incident energy and the kinematic factor for H⁺ on Sb, $K(\theta, M_1/M_2) E_0$, is drawn as a straight line in Fig. 2, where θ is the scattering angle and M_1/M_2 is the mass ratio of H to Sb. There are small measured intensity for exit angles less than 0° due to misdetections of the position sensitive detector. We could ignore these misdetections because the intensity is negligible and the angle resolution (FWHM) of the detector is less than 0.2° . The energies of the Sb peaks in the spectra are at every scattering angle smaller

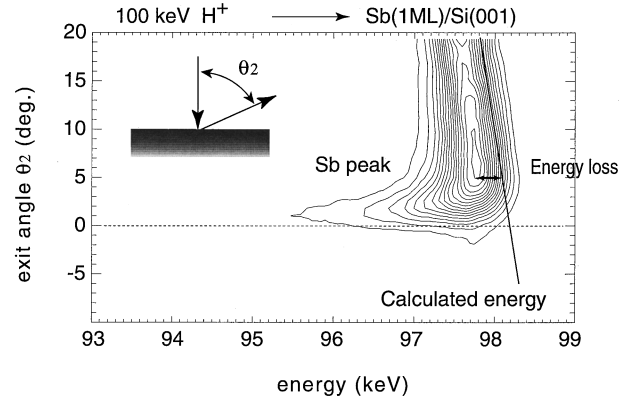


FIG. 2. A contour plot of a typical MEIS spectra set for 100.0-keV H⁺ incident along the [001] axis of the Si(001)2×1-Sb surface as a function of detected energy and scattering angle.

than the corresponding $K(\theta, M_1/M_2) E_0$ values. The energy difference is due to both the inelastic energy loss by excitation and/or ionization during the violent large-angle collision with an Sb atom and to continuous energy losses during the passage through the surface.

III. RESULTS

A. Energy loss

Figure 3 shows the energy spectra from the Sb atoms for the exit angles θ_2 of 75° , 80° , 87° , and 88° relative to the surface normal. Here, 100.0-keV H⁺ was incident along

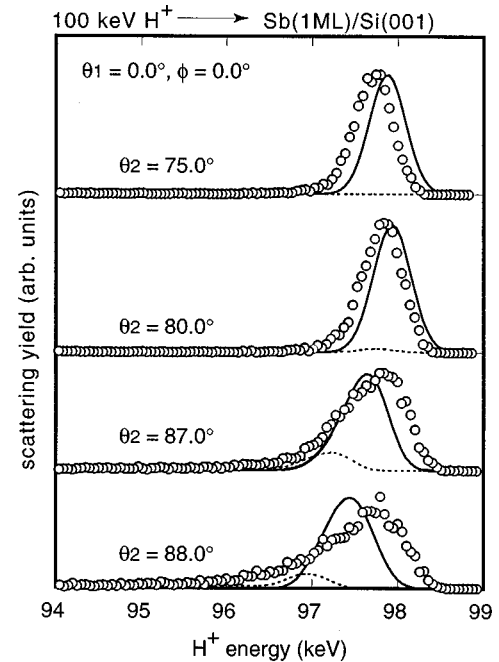


FIG. 3. Backscattering spectra from topmost Sb atoms on Si(001) for 100-keV H⁺ incidence ($\theta_1=0^\circ$, $\phi=0^\circ$) with exit angles θ_2 of 75° , 80° , 87° , and 88° . The solid curves denote the primary component without multiple scattering. The dashed curves denote the component of multiple scattering, defined here as a large-angle collision with a topmost Sb atom and subsequent small-angle collision with another Sb atoms.

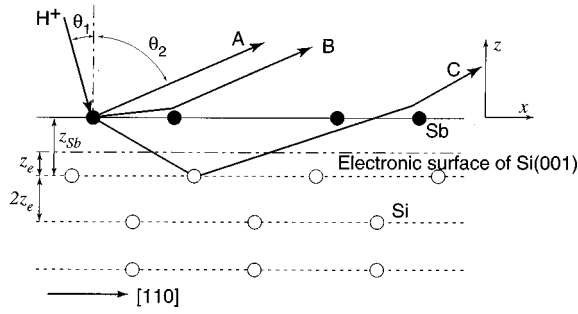


FIG. 4. Schematic illustration of various kinds of scattering events near the surface region of Sb (1 ML)/Si(001).

[001] ($\theta_1=0^\circ$) and the azimuth of the scattering plane, ϕ , relative to [110] was 0° . The Sb spectra at large exit angles clearly show asymmetric shapes with low-energy tails. With decreasing exit angles the profiles gradually become symmetric. These asymmetric profiles are possibly due to multiple scattering and the stochastic nature of inelastic collisions with the electrons of surface atoms.

In order to separate the contributions of multiple scattering from experimental Sb peaks, we performed Monte Carlo simulations. In our calculation, the projectile (H^+ ions) were generated at a position of the large-angle collision with a surface Sb atom by three normal random numbers considering the thermal lattice vibration. The emitted directions were defined by polar and azimuth angles, which were generated by two uniform random numbers. The exiting ion trajectories were followed up 3 \AA above the surface plane and then the final emission direction and energy were calculated. The ion was counted by weighting a coefficient considering the scattering. We used the universal (ZBL) interatomic potential¹⁹ and the impact-parameter-dependent stopping power of the Oen and Robinson model,²⁰ whose average value was normalized to the bulk Sb stopping power measured in advance. The thermal vibration amplitudes were derived from their Debye temperatures. The vertical component for the surface Sb was enhanced by a factor of $\sqrt{2}$ times that of the bulk value.

The dashed and solid curves in Fig. 3 correspond to the ion yields with and without additional scattering from neighboring Sb atoms. The multiply scattered ions travel a longer path in the crystal than the singly scattered ones. Consequently, they lose more energy inelastically. Although the elastic energy loss of the multiply scattered ions is actually less than that of singly scattered one, the difference of the elastic energy loss is much smaller than the inelastic one. Figure 4 illustrates three kinds of scattering events, (A) single scattering from an Sb atoms, (B) multiple scattering from Sb atoms, and (C) multiple scattering from Sb and Si atoms. We regard those events as multiple scattering if the additional scattering is about an angle larger than 2° . The 2° scattering from Sb corresponds to an impact parameter of about 0.15 \AA , which is comparable to the two-dimensional thermal vibrational amplitude of Sb. The intensities at the lower-energy region (less than 96 keV) of the spectra for large exit angles are due to the scattering event (C), though these intensities are so small that calculated curves are behind the experimental plots in Fig. 3. Using the Monte Carlo simulation, we estimated the contributions from (B) and (C) to total yield to be 25% for $100\text{-keV } H^+$ incidence (θ_1

$=0^\circ$, $\theta_2=88^\circ$, $\phi=0^\circ$). However, the results of the calculation showed that the energy of the ion scattered in the event (C) were $1.5\text{--}3 \text{ keV}$ lower than the Sb peak energy. It is so far from the peak that we can consider only the contribution of event (B), which is estimated to be about 15% of the total yield. In addition, it must be noted that its contribution to the average energy loss is 6% at most. The simulated Sb peak energies are lower than the experimental ones for the larger exit angles, but higher for the smaller exit angles. These differences are caused by misestimate of the Oen-Robinson model in our calculation and the impact parameter dependence will be described in more detail elsewhere. The situation is almost the same for 50-keV incidence.

We evaluate the average energy loss $\langle \Delta E \rangle = K(\theta, M_1/M_2) E_0 - \langle E \rangle$, where $\langle E \rangle$ is the average detected energy defined as

$$\langle E \rangle = \frac{\sum_i E_i Y_i}{\sum_i Y_i}, \quad (1)$$

where Y_i is the scattering yield from Sb at energy E_i . In order to correct for the contributions of the multiply scattered ions to the measured energy spectra, we applied the results of the Monte Carlo simulations. The Sb energy spectra for glancing exit are well approximated by appropriate asymmetric Gaussian shapes. As mentioned previously, the Oen-Robinson model does not give an exact expression of impact-parameter-dependent stopping powers. Thus the simulated Sb spectrum was shifted to coincide the simulated Sb peak positions with the observed ones. Then the shifted multiple-scattering component (B) was subtracted from the approximated asymmetric Gaussian spectrum. The ions scattered from underlying Si atoms after a large-angle collision with Sb [event (C)] did not affect the results of this fitting, because their energies are much lower than the peak energy. The error generated in the present treatment cannot be estimated precisely, but is small (roughly less than a few %).

Figure 5 shows the corrected energy losses as functions of the exit angle for $100\text{-keV } H^+$ incidence [$\theta_1=0^\circ$, (a) $\phi=0^\circ$ and (b) $\phi=30^\circ$]. The solid and dashed curves are best-fit results according to

$$\Delta E = a(1/\cos\theta_1 + 1/\cos\theta_2) + b, \quad (2)$$

where ΔE is the electronic energy loss (eV), a and b are fit parameters. Equation (2) is derived from the assumption that the energy loss depends only on the total length of the path traveled near the surface. The kinematic scattering factor is almost unity and the incoming and outgoing energies of H^+ can be regarded as equal within 2%.

B. Energy straggling

The energy straggling for 50- and $100\text{-keV } H^+$ ions passing through the Si(001) 2×1 -Sb surface was also measured as a function of exit angle. Figure 6 shows the energy spread (standard deviation) of the Sb spectra for $100\text{-keV } H^+$ incidence ($\phi=0^\circ$) approximated by asymmetric Gaussian profiles neglecting the low-energy tails for the large exit angles. Unfortunately, the present Monte Carlo simulation could not reproduce the shape of the experimental spectra. We cannot estimate the multiple-scattering component accurately, al-

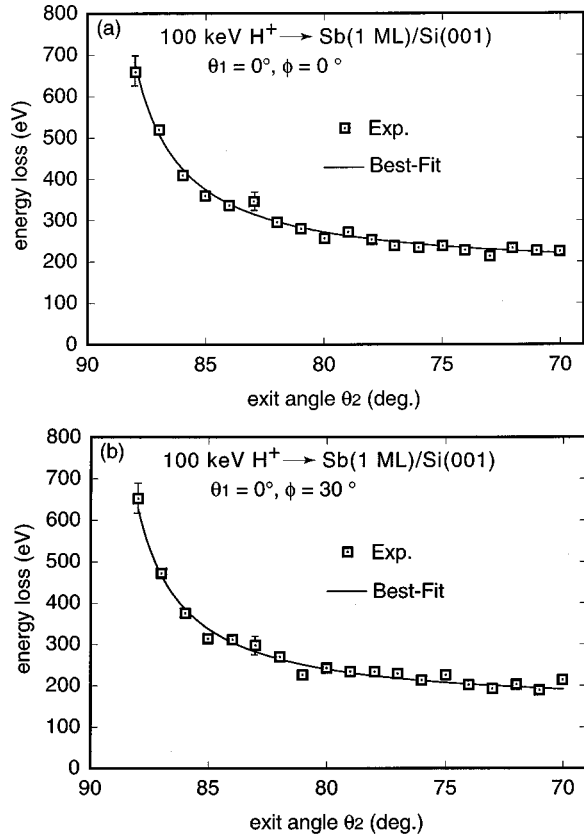


FIG. 5. Corrected energy loss as a function of exit angle for 100-keV H^+ incidence [$\theta_1 = 0^\circ$, (a) $\phi = 0^\circ$ and (b) $\phi = 30^\circ$]. The solid curves are fitted results.

though the multiple-scattering probably contributes to some extent. The solid curve is calculated in analogy to Eq. (2):

$$\Omega^2(\text{keV}^2) = a\{K^2/\cos\theta_1 + 1/\cos\theta_2\} + \Omega_{\text{SYS}}^2, \quad (3)$$

where $a(\text{keV}^2)$, K , and Ω_{SYS} are, respectively, a fitting parameter, the kinematic factor, and the system energy resolution (standard deviation). Equation (3) fits the measured energy straggling as a function of exit angle for 50- and 100-keV H^+ incidence ($\phi = 0^\circ$ and 30°) rather good. If one assumes that an ion which passes through the Sb surface

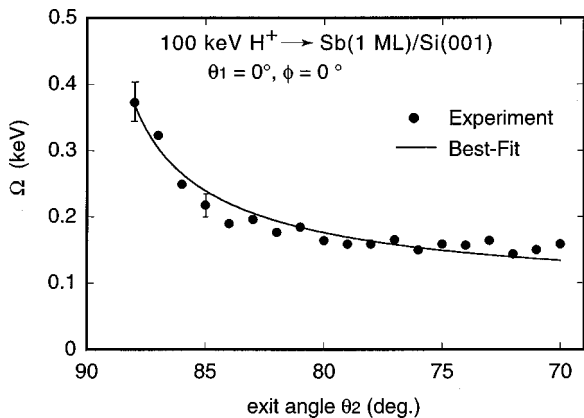


FIG. 6. Energy spread (standard deviation) of ions backscattered from topmost Sb atoms for 100-keV H^+ incidence ($\phi = 0^\circ$). Solid curve is fit of Eq. (3).

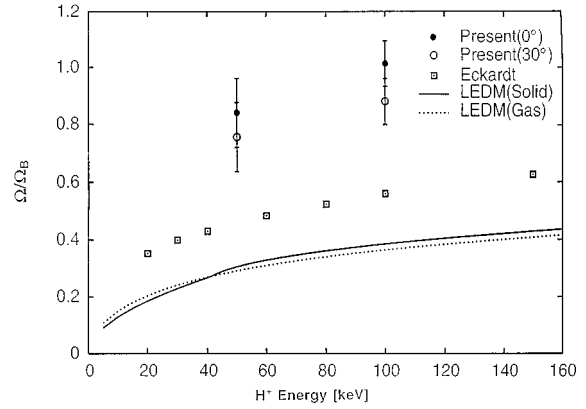


FIG. 7. Reduced straggling values (Ω/Ω_B) as a function of H^+ energy, where Ω_B is the Bohr straggling. The present data derived from the best-fit using Eq. (3) are plotted by full ($\phi = 0^\circ$) and open ($\phi = 30^\circ$) circles. The squares, solid, and dashed curves denote Eckardt's data (Ref. 21) solid-LEDM data, and gas-LEDM data, respectively.

layer experiences a constant energy spread (i.e., not a position dependent), our experimental a values can be compared with the straggling values for bulk Sb (Fig. 7). As frequently pointed out, it is essential to have a uniform and homogeneous thin film to measure the bulk energy straggling values precisely. We could not obtain a good accuracy in the straggling measurement because of the difficulty in preparing uniform Sb thin films on Si. Figure 7 compares our surface-energy straggling values with the experimental bulk data reported by Eckardt²¹ and with theoretical predictions based on the local electron-density model (LEDM's) of solid and gas models.^{23–25} The surface straggling values for $\phi = 0^\circ$ (in-plane) are significantly larger than those for $\phi = 30^\circ$ (off-plane), because the component due to multiple scattering is larger for $\phi = 0^\circ$. The surface-energy straggling values obtained corresponds with 0.8–0.9 of the Bohr straggling values, and are considerably larger than the bulk straggling values.

IV. DISCUSSION

We are attempting to delineate how much of the losses result from the plasmon. We are calculating the plasmon losses according to the theory, and then comparing the results to experimental losses. The contribution from surface-plasmon excitation can be estimated according to Kawai, Itoh, and Ohtsuki.⁸ Kitagawa⁹ derived the same expression, but using a different formulation. The calculated stopping power dE/dx (eV/cm) caused by the surface-plasmon excitation for 100-keV $H^+ \rightarrow \text{Si}$ is shown in Fig. 8 as a function of distance (z) from the Sb plane, where the electronic surface is taken as half of the interplanar distance outside the top Si layer.⁸ Here we used $\sqrt{\frac{5}{3}}\omega_p/\nu_F$ as the cutoff wave number, where ω_p and ν_F are the bulk plasma frequency and Fermi velocity, respectively, calculated assuming four free electrons per Si atom. The solid, dashed, and dot-dashed curves correspond to the total, surface, and bulk and reflective plasmon losses, respectively. The surface-plasmon loss for the outgoing path is given by

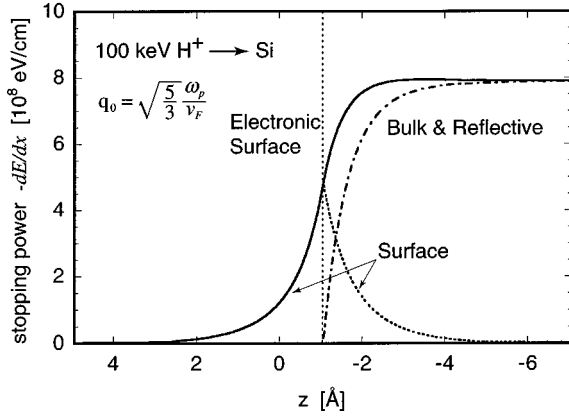


FIG. 8. Position-dependent plasmon losses for 100-keV H^+ incident on Si (calculated assuming four free electrons per Si atom). Solid, dashed, and dot-and-dashed curves denote total, surface, and bulk and reflectance plasmon losses, respectively.

$$\Delta E_S = \int_0^\infty \frac{dE}{dx}(z) dz = (\tan \theta_1 + \tan \theta_2) \int_0^\infty \frac{dE}{dx}(z) dz, \quad (4)$$

where we regard the Sb plane as the origin of the z axis (see Fig. 4).

The calculated plasmon loss for the present $H^+ \rightarrow \text{Si}(001)2 \times 1\text{-Sb}$ system was much smaller than the losses due to the collisions with the electrons of surface atoms. The small difference (less than 5%) between the calculated energy losses with and without the addition of surface-plasmon loss is within the experimental errors because of the large distance between the Sb and top Si layers (see Fig. 1). These situations are independent of the azimuthal angle and primary energy of the incidence beam. We regard the contribution of the surface-plasmon loss at the Si substrate surface as small enough in the present $H^+ \rightarrow \text{Si}(001)2 \times 1\text{-Sb}$ system, but it must be noted that the theories^{8,9} have ambiguities with regard to the cutoff wave number and the position of the electronic surface. The additional Sb surface-plasmon loss for 100-keV H^+ incidence cannot be estimated precisely but is likely less than 10%, though the real contribution of the deposited Sb atoms (1 ML) to the surface-plasmon loss is not clear at present.

The energy losses as a function of the exit angle are fit quite well by Eq. (2), as shown in Fig. 5 for 100-keV H^+ incidence. In the case of 50-keV H^+ , the relation is quite similar. Equation (2) is derived from the assumption that the energy loss depends only on the total length of the path traveled near the surface. In other words, we assume that the stopping is constant in a surface region up to d (cm) above the surface plane, and in that region it is not position dependent. Assuming a bulklike cutoff, $d = \sigma_{\text{Sb}}/2\rho_{\text{Sb}}$, where ρ_{Sb} and σ_{Sb} are the atomic density of bulk Sb and the areal density of the Sb monolayer on Si(001) ($6.78 \times 10^{14} \text{ cm}^{-2}$), respectively. When the stopping cross section of Sb is defined by $\varepsilon_{\text{Sb}} = (1/\rho_{\text{Sb}})dE/dx$ (10^{-15} eV cm^2),²⁶ the parameter a is theoretically equal to $\varepsilon_{\text{Sb}}\sigma_{\text{Sb}}/2$. The parameter b is the inelastic energy loss caused by the large-angle (92° – 110°) collision with Sb. The experimental values of a and b obtained by fitting are listed in Table I, where they are com-

TABLE I. Parameters a and b derived from experimental data and Eq. (2) by fitting and from the theoretical relation $a = \varepsilon_{\text{Sb}}\sigma_{\text{Sb}}/2$, where ε_{Sb} and σ_{Sb} are the stopping cross section of bulk Sb and the areal density of Sb on Si(001), respectively (units eV).

	100-keV H^+		50-keV H^+	
	$\phi=0^\circ$	$\phi=30^\circ$	$\phi=0^\circ$	$\phi=30^\circ$
	a	b	a	b
theory ($\varepsilon_{\text{Sb}}\sigma_{\text{Sb}}/2$)	16.0	16.0	16.6	16.6
expt.	18	150	17	125
			15	125
			15	150

pared with the theoretical values. The experimental values agree with $\varepsilon_{\text{Sb}}\sigma_{\text{Sb}}/2$ for the measured bulk Sb stopping cross sections within 9%.

Although we have assumed a sharp cutoff for stopping, it could actually be a bit different. A possible variation of the surface stopping power is exponential as a function of the distance from a top atomic plane. Such position-dependent stopping powers were determined from the surface-energy loss values measured with alkali-halide crystals under specular reflection conditions.^{27,28} Unfortunately, the specular reflection connected to the continuum potential of a surface atomic plane limits the distance from the surface plane more than about 0.3 \AA . It must be noted that the surface stopping powers derived here correspond to the integrated total stopping powers above the top atomic plane.

The surface stopping cross sections derived from the relation $a = \varepsilon_{\text{Sb}}\sigma_{\text{Sb}}/2$ are compared with the experimental data of Eckardt,²¹ the semiempirical formula given by Andersen and Ziegler,²² and the theoretical prediction of the LEDM,^{23,24} as shown in Fig. 9. The bulk stopping cross sections ε_{Sb} were measured separately for 50-, 65-, 80-, 100-, and 120-keV H^+ incident on $a\text{-Sb}$ (82 \AA)/Si(111). The thickness of Sb was measured by RBS with a 1.5-MeV He^+ beam and the surface roughness was quantitatively estimated with AFM. These experimental data are also plotted in Fig. 9. The

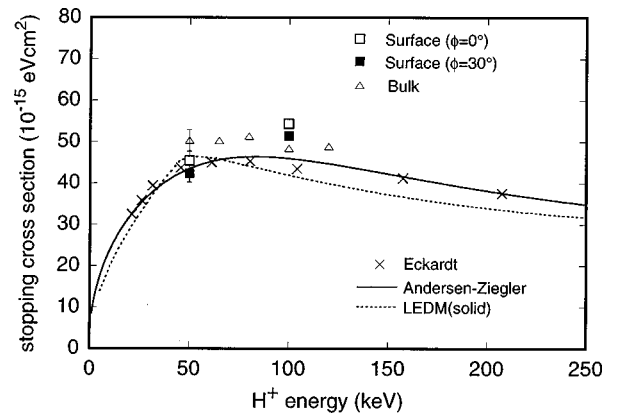


FIG. 9. Stopping cross section as a function of H^+ energy. The surface stopping cross section derived from Eq. (2) using the relation $a = \varepsilon_{\text{Sb}}\sigma_{\text{Sb}}/2$ are plotted by squares. For the stopping cross sections of Sb bulk, the triangles and crosses, respectively, denote the present data and the data reported by Eckardt (Ref. 21). The solid and dashed curves are, respectively, the semiempirical formula of Andersen and Ziegler (Ref. 22) and the calculated values based on the local electron-density model (LEDM) (Refs. 23 and 24).

present values, both the surface and the bulk, fit reasonably well with the above predictions. Thus, we come to the very useful conclusion that the average energy loss in the surface is given by the bulk stopping cross section and the areal density. The above relation suggests continuity of the stopping cross section from the bulk to the surface. We believe that a similar approach is possible in other systems as well. In order to determine the universality of this idea, we will discuss the surface-energy losses of another system in the near future, e.g., Ge/Si system in which surface segregation and intermixing phenomena will occur depending on annealing temperatures.

The surface-energy straggling as a function of the exit angle are also fit successfully by the simple relation with the total length of the path traveled near the surface. However, the surface straggling values obtained are significantly larger than those calculated from LEDM's, as shown in Fig. 7. This is partly due to the fact that the present straggling values include the contribution from the small-angle multiple scattering, which cannot be estimated accurately in the present Monte Carlo simulation. In addition, there exist a number of domain boundaries and the Sb dimers do not completely cover the Si-substrate surface, as expected from the scanning tunneling microscopy observation of the Si(001)2×1-Sb.¹⁵ In the present glancing emergence conditions, this may generate an additional contribution to surface-energy straggling. The electronic transitions which occur during the large-angle violent collision with the topmost Sb atom are a statistical process and thus also contribute to the energy spread of the exit ions. Unfortunately, it is very difficult to estimate this contribution quantitatively.

V. SUMMARY

The surface stopping cross sections and energy straggling were measured, with an electrostatic toroidal analyzer, for 50- and 100-keV H⁺ ions passing through the Si(001)2×1-Sb surface. To estimate the multiple-scattering contribution, we performed a Monte Carlo simulation of the trajectories of backscattered ions. The multiple-scattering contribution, including the component of ions scattered from substrate Si atoms, decreases with decreasing exit angle. At large exit angles the contribution is significantly larger when

$\phi=0^\circ$ than when $\phi=30^\circ$. In an off-plane ($\phi=30^\circ$) scattering geometry, the contribution from multiple scattering can be neglected. The contribution from surface plasmons excited at the Si substrate was estimated according to the methods of Kawai, Itoh, and Ohtsuki⁸ and Kitagawa⁹ and was found to be negligibly small in the present system.

The energy losses as a function of the exit angle are fit successfully by the simple relation with the time spent near the surface. The energy loss is given by the product of the bulk Sb stopping cross section and the areal Sb density: $\varepsilon_{\text{Sb}}\sigma_{\text{Sb}}/2$ (and note that the factor 2 stems from the fact that only the outerhalf of the Sb monolayer is traversed) plus the extra inelastic energy loss in the backscattering collision. This result suggests continuity of the stopping power from the bulk to the surface. It provides support for the use of the energy loss to measure the distance between a plane of deposited atoms and the first substrate plane; e.g., for the case of Ag on Si(001).⁶ In addition, it would make it possible to determine the elemental composition of each atomic layer of a subsurface region.

The energy straggling was also measured for the Si(001)2×1-Sb surface. The energy spread values (standard deviation) obtained assuming asymmetric Gaussian profiles are well fit by the relation with the square root of the total length of the path traveled near the surface. We found that the measured straggling in the surface was considerably larger than in Sb bulk, as measured by Eckhardt²¹ or predicted by theory.²³⁻²⁵ This is partly due to the fact that our straggling values include contributions from the small-angle multiple scattering and from domain boundaries of Sb dimers. It is also suggested that the electronic transitions which occurred during the backscattering process may contribute to the energy spread of the exit ions.

ACKNOWLEDGMENTS

We thank Dr. T. Ogino of NTT Basic Research Laboratory for support throughout the present work. We would also like to acknowledge the valuable discussions we had with Professor T. Koshikawa and Professor T. Yasue of Osaka Electrocommunication University. Special thanks are due to M. Honda and T. Nishimura for assisting with the Monte Carlo simulation and for preparing the illustrations.

*Present address: NTT Opto-electronics Laboratories, Atsugi, Kanagawa 243-01, Japan.

¹J. F. van der Veen, Surf. Sci. Rep. **5**, 199 (1985).

²J. Vrijmoeth, P. M. Zagwijn, J. W. M. Frenken, and J. F. van der Veen, Phys. Rev. Lett. **67**, 1134 (1991).

³M. Copel and J. Falta, Phys. Rev. B **48**, 2783 (1993).

⁴T. Koshikawa, T. Yasue, H. Tanaka, I. Sumita, and Y. Kido, Surf. Sci. **331-333**, 506 (1995).

⁵K. Sumitomo, T. Nishioka, and T. Ogino, Appl. Surf. Sci. **100/101**, 503 (1996).

⁶K. Kimura, K. Ohshima, and M. Mannami, Phys. Rev. B **52**, 5737 (1995).

⁷J. F. Ziegler, *Helium Stopping Powers and Ranges in All Elements* (Pergamon, New York, 1977).

⁸R. Kawai, N. Itoh, and Y. H. Ohtsuki, Surf. Sci. **114**, 137 (1982).

⁹M. Kitagawa, Nucl. Instrum. Methods Phys. Res. B **33**, 409 (1988).

¹⁰K. Kimura, M. Hasegawa, and M. Mannami, Phys. Rev. B **36**, 7 (1987).

¹¹Y. Fujii, S. Fujiwara, K. Narumi, K. Kimura, and M. Mannami, Surf. Sci. **277**, 164 (1992).

¹²Y. Fujii, K. Kishine, K. Narumi, K. Kimura, and M. Mannami, Phys. Rev. A **47**, 2047 (1993).

¹³K. Narumi, Y. Fujii, K. Kishine, S. Fujiwara, K. Kimura, and M. Mannami, J. Phys. Soc. Jpn. **62**, 1603 (1995).

¹⁴R. Nunez, P. M. Echenique, and R. H. Ritchie, J. Phys. C **13**, 4229 (1980).

¹⁵M. Richter, J. C. Woicik, J. Nogami, P. Pianetta, K. E. Miyano, A. A. Baski, T. Kendelewicz, C. E. Bouldin, W. E. Spicer, C. F. Quate, and I. Lindau, Phys. Rev. Lett. **65**, 3417 (1990).

¹⁶A. Ishizaka and Y. Shiraki, J. Electrochem. Soc. **133**, 666 (1986).

¹⁷S. A. Barnett, H. F. Winters, and J. E. Greene, Surf. Sci. **165**, 303 (1986).

- ¹⁸S. Tang and A. J. Freeman, Phys. Rev. B **74**, 1460 (1993).
- ¹⁹J. F. Ziegler, J. P. Biersack, and W. Littmark, *The Stopping and Range of Ions in Matter* (Pergamon, New York, 1985).
- ²⁰O. S. Oen and M. T. Robinson, Nucl. Instrum. Methods **132**, 647 (1976).
- ²¹J. C. Eckardt, Phys. Rev. A **18**, 426 (1978).
- ²²H. H. Andersen and J. F. Ziegler, *Hydrogen Stopping Powers and Ranges in All Elements* (Pergamon, New York, 1977).
- ²³I. Gertner, M. Meron, and B. Rosner, Phys. Rev. A **18**, 2022 (1978).
- ²⁴T. Kaneko, Phys. Rev. A **33**, 1602 (1986).
- ²⁵Y. Kido and T. Koshikawa, Phys. Rev. A **44**, 1759 (1991).
- ²⁶L. C. Feldman and J. W. Mayer, *Fundamentals of Surface and Thin Film Analysis* (Elsevier Science, New York, 1986).
- ²⁷Y. Fujii, S. Fujiwara, K. Narumi, K. Kimura, and M. Mannami, Surf. Sci. **277**, 164 (1992).
- ²⁸Y. Fujii, K. Narumi, K. Kimura, and M. Mannami, Nucl. Instrum. Methods Phys. Res. B **67**, 82 (1992).